International Council for the Exploration of the Sea

CM 1999/K:03
Theme Session on Application of Coupled Bio-Physical Models in Studies of Zooplankton and Ichtyoplankton Advection and Dispersion

Modelling the advection and diffusion of eggs and larvae of northeast Arctic Greenland halibut

Bjørn Ådlandsvik[*], Agnes C. Gundersen[†], Kjell H. Nedreaas[*], Anne Stene[‡], and Ole T. Albert[§],

Abstract

In later years there has been considerable uncertainty on the recruitment of the northeast Arctic stock of Greenland halibut (*Reinhardtius hippoglossoides*). The abundance of several year classes originally considered very low at 0-3 years age, are now considered higher than expected at the age of 6 or more. A possible explanation, raised earlier, is more northeasterly than expected distribution of the young fish by active migration and/or drift of eggs and larvae.

The present work considers the transport and dispersion of eggs and larvae of Greenland halibut by numerical modelling. Current fields from a 3D baroclinic hydrodynamic model are fed in to a Lagrangian particle tracking model. The particles are released into the current at the spawning field along the shelf slope from Vesterålen to Bjørnøya (69-75°N). Vertically, the particles can follow a predefined depth-by-age curve or be kept at a fixed depth. This model system is used for different years to examine changes in the drift pattern.

[*]Institute of Marine Research, P O.Box 1870 Nordnes, N-5817 Bergen
[†]Møre Research, Section of Fisheries, P.O.Box 5057, N-6021 Ålesund
[‡]Ålesund College, P.O.Box 5104, N-6021 Ålesund
[§]Norwegian Institute of Fisheries and Aquaculture Ltd. (Fiskeriforskning), N-9291 Tromso

1 Introduction

Northeast Arctic Greenland halibut (*Reinhardtius hippoglossoides* Walbaum) is distributed in the Norwegian and Barents Sea, mainly on the continental slope off Norway from 62°N to the regions north of Spitsbergen. The Northeast Arctic Greenland halibut constitutes a separate management unit in the ICES management system. A drop in year-class indices derived from the regular 0-group and juvenile surveys was observed in the late 1980s. At the same time a historic low spawning stock biomass was observed (Hylen & Nedreaas, 1995; Smirnov, 1995). The importance of Greenland halibut as a commercial fish species increased during the same period, but a decrease in the commercial catch per unit of effort (CPUE), low spawning biomass, and the drop in recruitment indices led to strong regulations including a fishing ban north of 71°30'N from 1992.

Based on extremely low catch rates in the surveys, the yearclasses born in the beginning of the 1990s were considered very poor. New results indicate that the 1990–92 yearclasses may be at the same level as those prior to the previously assumed recruitment failure (ICES, 1999). The reason for this change in catchability is not clear. However, it seems clear that important areas for young Greenland halibut may be found north and east of Svalbard (Gundersen *et al.*, 19xx).

Albert *et al.* (1997) showed that the south-western end of the distribution area of age 1 fish was gradually displaced northwards along west Spitsbergen in the period 1989–92 and southwards in the period 1994–96. These displacements corresponded to changes in hydrography and may be explained by increased migration of the 1989–92 yearclasses to areas outside the areas covered by the surveys.

Northeast Arctic Greenland halibut is distributed down to 1400 m depth. However, in other parts of the Atlantic, Greenland halibut is observed down to 2000 m (Boje & Hareide, 1993). Greenland halibut is described as a boreal-arctic species and is mainly found at temperatures between -1°C and +4°C. Recent studies on the spawning biology of Northeast Arctic Greenland halibut conclude that the main spawning season is from November to mid January. Peak spawning is in December (Albert *et al.*, 1998). Spawning is mainly believed to occur along the continental slope between Lofoten and Bear Island. The larvae drift with the currents and are found as 0-group, mainly in the waters west and north of Spitsbergen in August-September (e.g. Anon (1996)). Older juveniles are observed around Spitsbergen until the age of 3-5. Main nursery areas are so far observed to be between Hopen Island and King Karl Land / White Island and in the Hinlopen Strait between Spitzbergen and Nordaustlandet (Gundersen *et al.*, 19xx).

This paper consider the transport phase of eggs and larvae of northeast Arctic Greenland halibut. The problem is to describe the transport pattern and its variability. Some causes for variability such as inter-annual variability in the physical environment, variability in spawning pattern and transport depth are also considered. Variability due to differences in survival conditions are not considered.

The method used is numerical modelling. In recent years this technique has been used to study the transport and dispersion of eggs and larvae of several fish stocks. This is usually done by a combination of a regional hydrodynamic current model producing current fields and a Lagrangian particle tracking model for transport and dispersion. At the Institute of Marine Research (IMR) this technique has been used for several stocks; for North Sea sandeel (Berntsen *et al.*, 1994), Arcto-Norwegian cod (Ådlandsvik & Sundby, 1994), Norwegian spring-spawning herring (Svendsen *et al.*, 1995), Barents Sea polar cod (Hansen &

Ådlandsvik, 1996), Barents Sea capelin (Eriksrød & Ådlandsvik, 1997), and blue whiting (Skogen *et al.*, 1999).

2 Modelled current fields

The transport model is driven by the input current fields. The quality of the particle trajectories is therefore limited by the quality of the current field. An understanding, of the strengths and weaknesses of the current field, is a prerequisite for a proper interpretation of the particle transport.

2.1 The hydrodynamic model

The numerical model used is based the well-known Princeton Ocean Model (POM) developed by (Blumberg & Mellor, 1987) with modifications done at The Norwegian Meteorological Institute (DNMI) and the Institute of Marine Research (IMR). This is a 3D baroclinic ocean model, with surface elevation, velocity, salinity, temperature and two variables for vertical mixing as model variables. In addition to the initial and boundary description of the model variables, the model forcing may include wind stress, air pressure, heat exchange with the atmosphere, tidal forcing, and river run-off.

The model solves the primitive equations numerically by the finite differences method. In the vertical, bottom following σ-coordinates are used. The model uses mode splitting between the external gravity wave mode and the internal baroclinic mode. The leapfrog technique is used to step forward in time. For vertical mixing a level 2.5 Mellor-Yamada turbulence closure scheme is used (Mellor & Yamada, 1982).

2.2 Model set-up

The initial description of sea surface elevation, currents, salinity and temperature is taken from the DNMI-IMR diagnostic climatology, (Engedahl, 1995). At the open boundaries this is complemented by the four tidal constituents. The meteorological forcing is taken from the hindcast archive of DNMI, (Eide *et al.*, 1985). This archive have a temporal resolution of six hours and a spatial resolution of 75 km. In lack of data on heat exchange between the ocean and atmosphere, the surface temperature is relaxed towards the climatology. The precipitation minus evaporation is set to zero. Freshwater outflow from 47 rivers (20 Norwegian) is included.

The polar stereographic model domain is shown in figure 1. The spatial resolution is 20 km. In the vertical 14 σ-levels were used. The simulations were started from the same climatological initial field for each of the 4 years 1988-1991, with a spin-up time from 15 November the preceding year. To remove the tidal signal, the results were filtered by daily 25 hour averages.

2.3 Current results

As an example, figure 1 shows the averaged surface current field for April 1989. The main current in the picture is the Norwegian Atlantic Current entering the Norwegian Sea through the Faroe-Shetland channel and northwest of the Fareos. Inside the Norwegian Sea it follows the shelf break west of Norway. The current has two major splitting areas. The first area is

outside northern Norway with one branch entering the Barents Sea and the other continuing along the shelf break towards the Fram Strait area west of Spitsbergen. Here, one branch enters the Arctic Ocean flowing eastwards along the Barents shelf break while the other branch turns towards the Greenland shelf and ends up as part of the East Greenland Current. Atlantic water may enter the Barents Sea from north, but this was not reproduced by the model this month. Overall, the modelled current field compares well with standard views of the circulation in the area, see e.g. Hansen *et al.* (1998); Poulain *et al.* (1996).

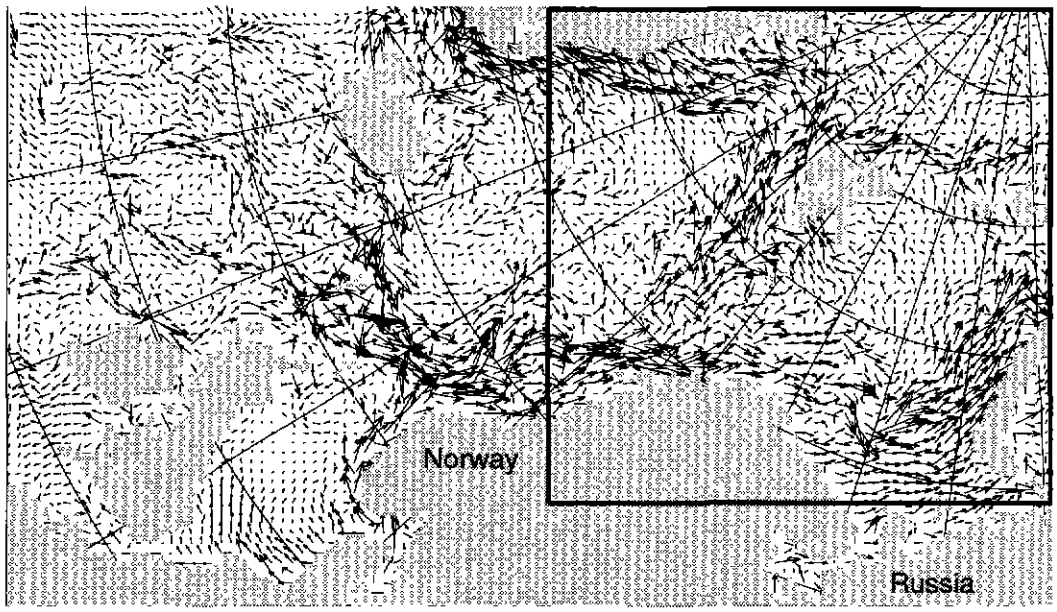

Figure 1: Model area with averaged modelled surface current for April 1989. Also shown is the subarea for particle tracking.

3 Particle tracking

3.1 Model

The Lagrangian Advection and Diffusion Model (LADIM) is a particle tracking transport model developed at IMR. A full documentation of this model will be given in (Ådlandsvik, 1999).

The input data to the transport model is a gridded current field, usually time dependent. Passive particles are released into the current field. Advection is simulated by moving the particles forward with the current at discrete time steps, i.e. an Euler Forward scheme. Shear in the current field tends to spread the particles. Additional diffusion may be simulated by "random walk" i.e. giving the particles a random jump each time step. If a particle would hit land during the next time step by the procedure above, its position will be unchanged.

Vertically the depth of a particle is prescribed, either as a fixed depth or more generally following a depth-by-age curve. If a particle hits the bottom, its depth is adjusted to 99%

of the bottom depth. If it reaches deep enough water later on, the depth is reset to the prescribed value.

3.2 Sensitivity studies

To understand the behaviour of a transport model it is necessary to perform some sensitivity studies. Here, this is done by providing a standard run and to examine how variations in spawning time, transport depth and spawning location influences the particle distributions.

3.2.1 The standard run

In the standard run, particles are released at 10 locations along the 600 m isobath as shown in fig 2. At each location 100 particles are released 1. January 1989. The particles are held at a fixed depth of 300 m. The random walk diffusion corresponds to an eddy diffusion coefficient of $100\,\mathrm{m^2 s^{-1}}$. This value were suggested in (Ådlandsvik & Sundby, 1994) as reasonable for spreading of cod larvae in the Barents Sea.

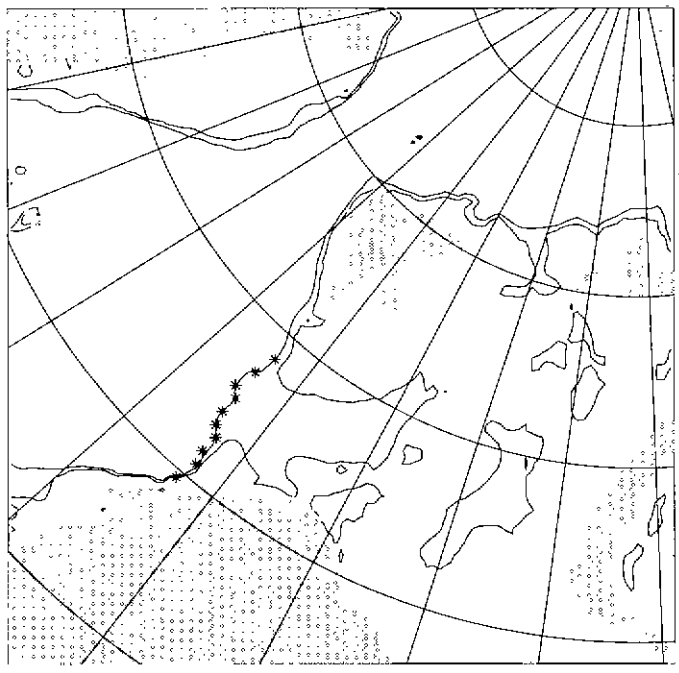

Figure 2: Particle release locations in the standard run. Also shown are the 300 m and 600 m isobaths

The results from this simulation is presented in figure 3 as time slices every 50th day. The particle distribution soon splits up with one patch entering the Barents Sea at the southern flank of the Bear Island Trench. Here it is trapped by the 300 m isobath and continues cyclonically in the trench. Another patch of particles travels northwards and turns east north of Spitsbergen. Most of these particles leave the model domain northeast of Franz Josef Land. In this run, only a single particle reaches the east Greenland shelf.

To obtain a more quantitative analysis, the domain is subdivided into non-overlapping areas. The Barents Sea area is limited in west by 20°E and in north by 77°N. The Norwegian

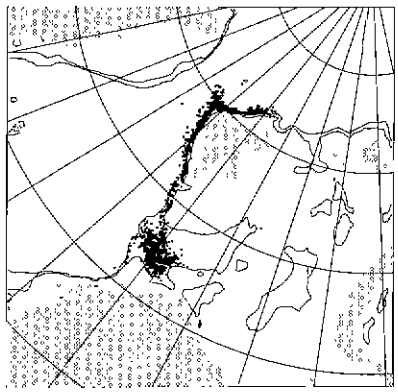

(a) 50 days

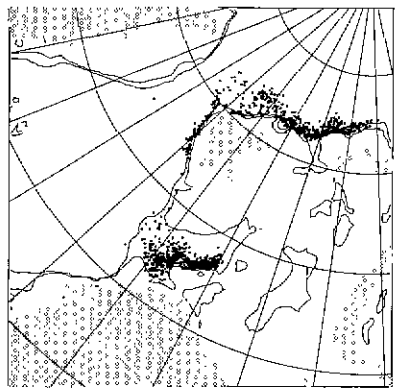

(b) 100 days

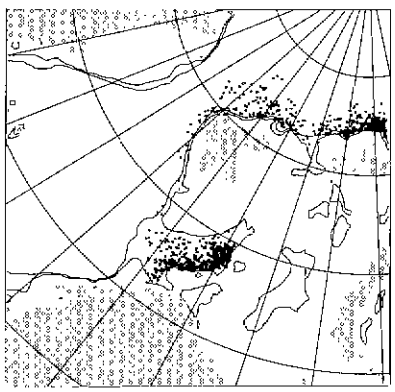

(c) 150 days

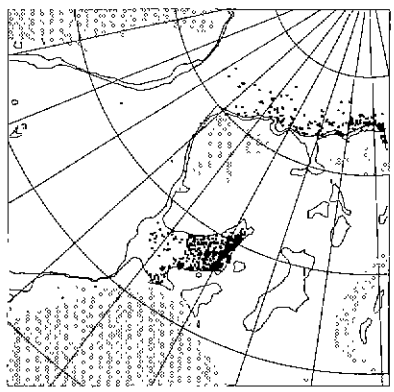

(d) 200 days

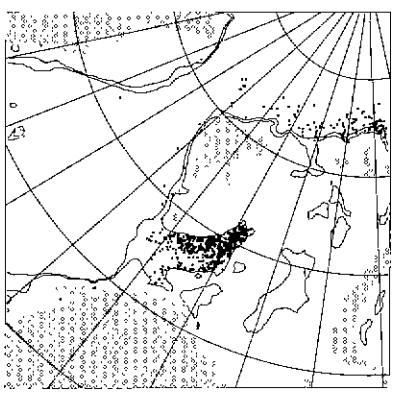

(e) 250 days

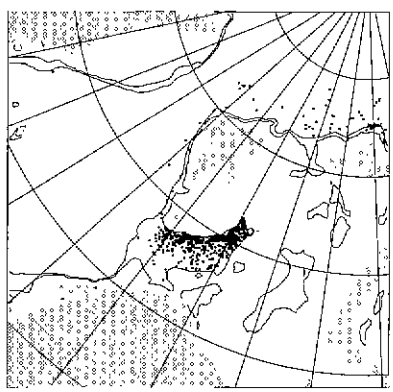

(f) 300 days

Figure 3: Particle positions from the standard run

Time	Lost	Norwegian	Barents	Greenland	Arctic
0	0	1000	0	0	0
50	0	604	246	0	150
100	0	146	430	1	423
150	90	44	465	1	400
200	294	22	462	1	221
250	395	22	459	1	123
300	464	45	434	1	56

Table 1: Number of particles in different categories in the standard run

Time	Lost	Norwegian	Barents	Greenland	Arctic
0	0	1000	0	0	0
50	0	869	127	0	4
100	0	316	397	0	287
150	0	128	473	1	398
200	107	70	476	1	346
250	283	66	467	1	183
300	370	52	465	1	112

Table 2: Number of particles in different categories with particle release 1. February 1989 and fixed transport depth of 300 m

Sea area lies between 0°E and 20°E and is limited in north by 80°N. The Greenland Sea area is limited in east by 0°E and in north by 80°N. The rest of the domain belong to the Arctic Ocean area. The special northern border of the Barents Sea is chosen so that particles entering from north are counted as arctic. The lost particles are here treated as a separate area, but could be added to the arctic category.

The particle counts in these areas are presented in table 1. Initially all particles belong to the Norwegian Sea, but after 100 days nearly half the particles have entered the Barents area and a similar number have reached the Arctic area. Thereafter the arctic particle count diminishes as particles leaves the domain. After 300 days, there are 520 arctic particles (including the lost ones). The Barents Sea count drops a little towards the end of the simulation period as particles reenters the Norwegian Sea at the northern flank of the trench.

3.2.2 Dependence on spawning time

Particles released at different time will not have identical trajectories, due to the current field being time dependent. This is tested, first by postponing the particle release for one month and thereafter by following a more realistic spawning curve.

Figure 4 shows the particle distributions after 50 and 200 days from a simulation with spawning time 1. February as the only difference from the standard run. The results look very similar to the standard run. Quantitatively, the results are summed up in table 2. This show a similar near equal splitting between Barents and Arctic particles. The main difference is less loss of particles.

With a time dependent spawning intensity curve, the first particles are released 1. December, main spawning in mid January and a decreased spawning towards the end of February.

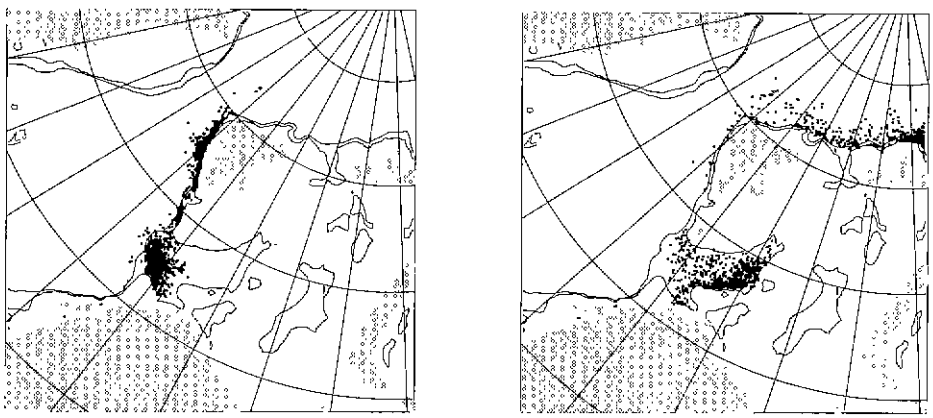

(a) 50 days (b) 200 days

Figure 4: Particle positions from simulation starting 1. February 1989 with fixed depth of 300 m

Time	Lost	Norwegian	Barents	Greenland	Arctic
0	0	20	0	0	0
50	0	792	18	0	0
100	0	571	228	3	198
150	8	225	397	3	367
200	125	56	451	3	365
250	249	29	452	3	267
300	397	27	448	3	125

Table 3: Number of particles in different categories with spawning time curve and fixed transport depth 300 m

The results are not immediately comparable to the standard run, as the mean transport time is 40–50 days less than the transport time recorded for the earliest particles. Figure 5 shows the result after 50 and 200 days and table 3 shows the particle counts. These results show the same overall pattern as the standard run and the 1. February run. Quantitatively, the results are more similar to the 1. February run.

3.2.3 Dependence on transport depth

Knowledge of vertical distribution is essential in understanding the horizontal transport of fish eggs and larvae. For eggs the vertical distribution is determined by the buoyancy, the diameter and the vertical mixing. In contrast to pelagic eggs, the vertical spreading of bathypelagic eggs at equilibrium conditions depends mostly on the buoyancy. A large difference in the vertical distribution is expected between the heaviest and lightest fraction of an egg population (Sundby, 1991).

Eggs from the Northeast Arctic population were registered in the Barents Sea for the first time in December 1997 (Albert *et al.*, 1998).

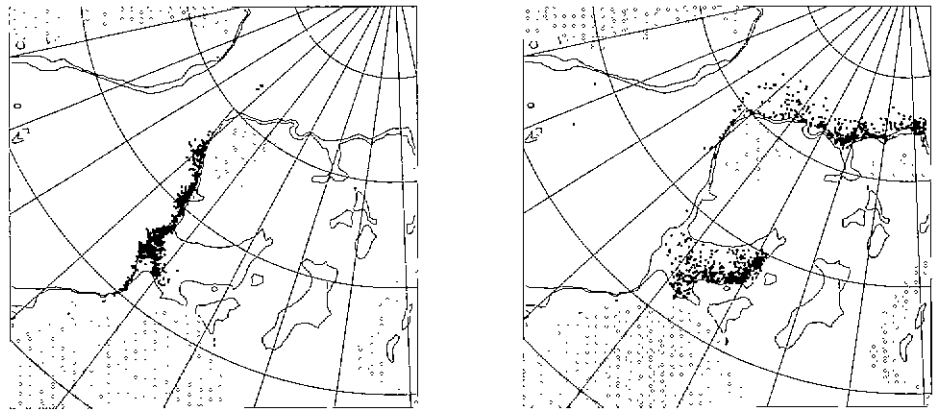

(a) 50 days (b) 200 days

Figure 5: Particle positions from spawning time curve simulation with fixed depth of 300 m

In Atlantic halibut it is reported significant differences in egg diameter between different areas and between sampling years at the same spawning location (Haug *et al.*, 1984).

The eggs of Greenland halibut have a small perivitelline space. This may indicate no subjection to sudden accelerates forces, and an adaptation to a bathypelagic distribution (Forrester & Alderdice, 1973).

The salinity of the surface water in the spawning area was measured to be 35.0 psu (ca 5°C, depth of 5 m). In this sea-water artificially fertilized eggs had full buoyancy during the first days of development (Stene *et al.*, 1999). At 5°C artificially spawned eggs had neutral buoyancy in salinities of 31.2 to 34.0 psu and sank to the bottom in salinities below 31 psu. This large buoyancy and the large diameter of the eggs give raising velocities of several mm/s (see Sundby (1983)). This will bring the eggs near the surface in few days.

During gastrulation the egg density increased, stabilizing at salinities of 35.5 psu ca 2°C after closure of blastopore. At 5°C neutral buoyancy salinity of eggs from the field survey was 35.2 psu. This weaker negative buoyancy will give a slower sinking of the eggs. Neutral buoyancy salinities determined in the laboratory upon artificially fertilized eggs of Atlantic halibut, were also higher than the buoyancy salinities of eggs from field surveys (Lønning *et al.*, 1982). The neutral buoyancy salinity of Greenland halibut eggs from field surveys corresponds to a sea-water density of ca 1027.9 kgm^{-3}. This density is found at depths around 650 meters (34.9 psu and 1.8°C) in the spawning area.

In June–July, 0-group of northeast Arctic Greenland halibut are found at depths of 50–60 m (Haug *et al.*, 1989).

The data available are not sufficient to produce a realistic depth-by-age curve. The variability may also be too large for such a curve to be meaningful. On the other hand, the model need a depth every time step. The depth-by-age curve presented in figure 6, must be considered only as an example of vertical behaviour consistent with the sparse information on the subject.

The transport with a fixed depth of 50 m is presented in figure 7 and table 4. Here most of the particles enter the Barents Sea, with a much wider distribution. Also a substantial part of the Arctic particles enters the Barents Sea from north. The loss of particles is drastically

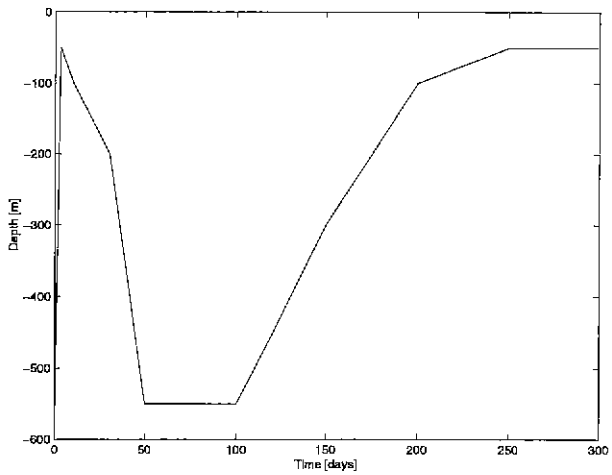

Figure 6: Depth curve

Time	Lost	Norwegian	Barents	Greenland	Arctic
0	0	1000	0	0	0
50	0	277	673	0	50
100	0	85	785	0	130
150	9	52	805	0	134
200	20	43	807	0	130
250	27	36	812	0	125
300	36	23	812	0	129

Table 4: Number of particles in different categories with transport depth 50 m

reduced from the standard run.

The results with a fixed transport depth of 600 m is presented in figure 8 and table 5. As the depth of the Barents Sea is shallower than 600 m, no particles enters this area. Most particles goes into the Arctic, but due to lower velocities, the loss from the area is less than in the standard run. The number of particles in the Greenland sector is increased. Also note that some of the Arctic particles are close to the Greenland shelf.

A simulation was performed where the depth varied in time according to the depth curve in figure 6. The results are shown in figure 9 and table 6. During the first near surface phase, a large portion of the particles enters the Barents Sea. In the following deeper phase, the spreading in the Barents Sea is delayed. The other near half of the particles ends up in the Arctic, with a few particles entering the Barents Sea from north during the final shallow phase.

3.2.4 Dependence on spawning location

The dependence of spawning location is first examined by looking at the southern and northern fraction of the particles in the standard run.

The results from the five southernmost positions are given in figure 10 and table 7. Nearly 80% of these particles are found in the Barents Sea.

The results from the five northernmost particle release locations are presented in figure 11

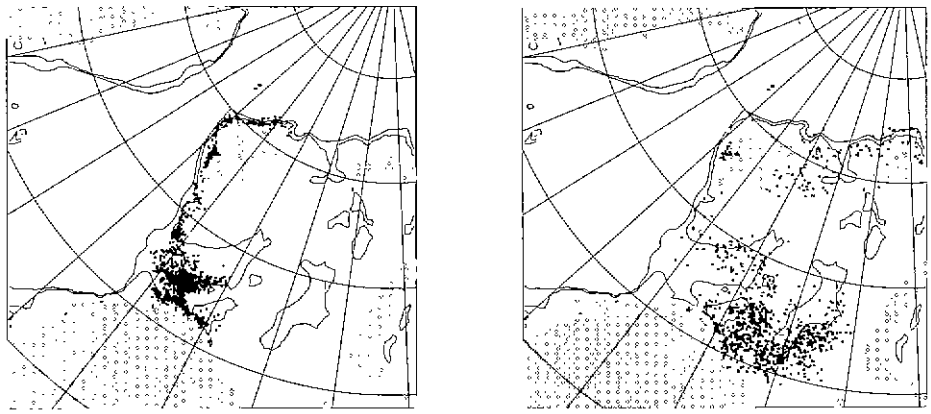

(a) 50 days (b) 200 days

Figure 7: Particle positions from simulation with fixed depth of 50 m

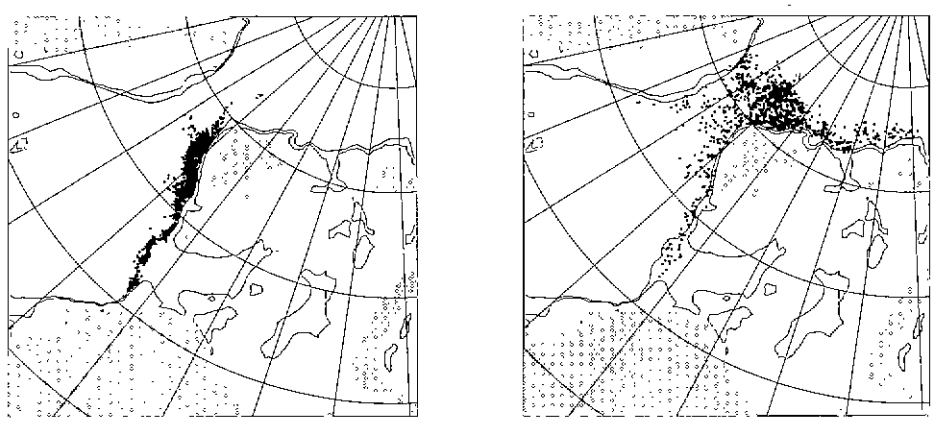

(a) 50 days (b) 200 days

Figure 8: Particle positions from simulation with fixed depth of 600 m

Time	Lost	Norwegian	Barents	Greenland	Arctic
0	0	1000	0	0	0
50	0	998	0	0	2
100	0	639	0	11	350
150	0	351	0	31	618
200	0	180	0	29	791
250	30	113	0	35	822
300	108	76	1	34	781

Table 5: Number of particles in different categories with transport depth 600 m

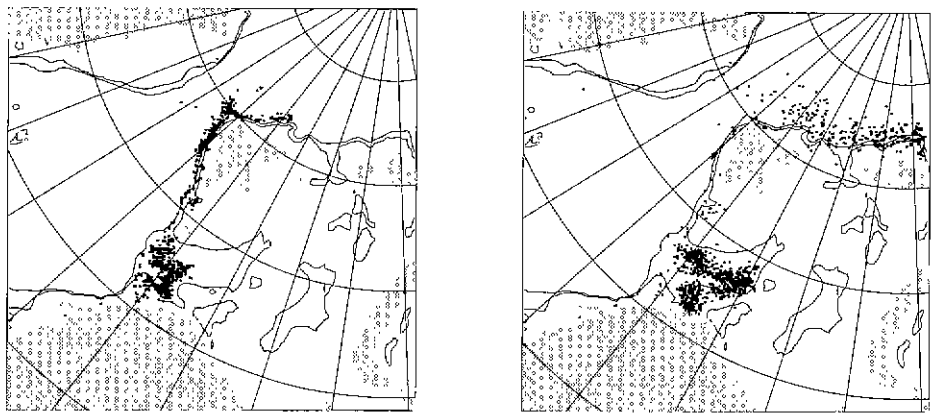

(a) 50 days (b) 200 days

Figure 9: Particle positions from simulation with depth varying in time

Time	Lost	Norwegian	Barents	Greenland	Arctic
0	0	1000	0	0	0
50	0	526	387	1	86
100	0	246	453	2	299
150	20	150	515	2	313
200	99	76	553	3	269
250	178	35	582	4	201
300	236	17	595	5	147

Table 6: Number of particles in different categories with time varying depth

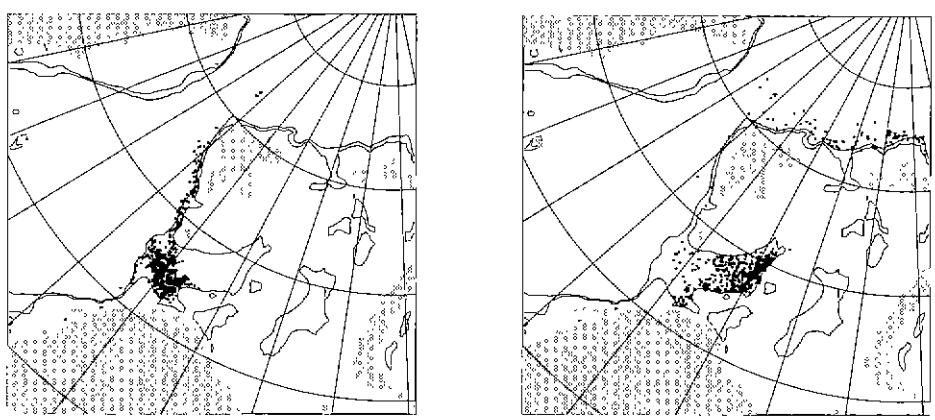

(a) 50 days (b) 200 days

Figure 10: Particle positions from the 5 southern locations in the standard run

Time	Lost	Norwegian	Barents	Greenland	Arctic
0	0	500	0	0	0
50	0	291	209	0	0
100	0	110	363	0	27
150	0	38	395	0	67
200	6	17	395	0	82
250	39	16	393	0	52
300	69	35	372	0	24

Table 7: Number of particles from south in the standard run

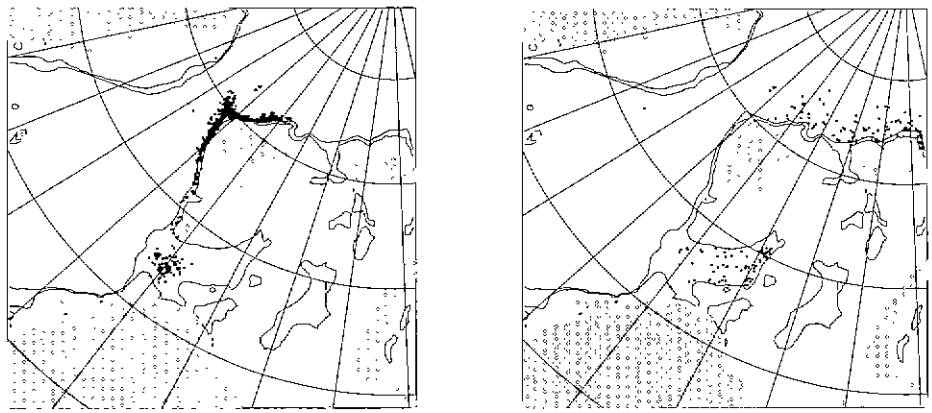

(a) 50 days

(b) 200 days

Figure 11: Particle positions from the 5 northern locations in the standard run

and table 8. Here approximately 85% of the particles goes into the Arctic. After 300 days nearly 80% of the particles have left the domain.

Another variation of the standard run were performed with release locations a little further offshore, over the 800 m isobath. The results are presented in figure 12 and table 9. Compared with the standard run, the particle count in the Barents Sea is decreased with a similar increase in the Arctic. The number of particles reaching the Greenland shelf has increased, but is still low.

3.3 Interannual variability

The standard run has been repeated with the current fields for 1988 and 1990–91, giving a total simulation time of four years. The results from 1988 are presented in table 10 and figure 13. The results from 1990 in table 11, figure 14, and the 1991 results in table 12, figure 15.

Table 13 shows the particles of each category after 300 days for each of the years. Note that the lost particles are here counted as Arctic. The last column consist of the modelled wind driven winter inflow to the Barents Sea. This has bee done by a simpler barotropic model Ådlandsvik & Loeng (1991). Based on the 30 years 1970-99 the mean winter inflow

Time	Lost	Norwegian	Barents	Greenland	Arctic
0	0	500	0	0	0
50	0	313	37	0	150
100	0	36	67	1	396
150	90	6	70	1	333
200	288	5	67	1	139
250	356	6	66	1	71
300	393	10	62	1	32

Table 8: Number of particles from north in the standard run

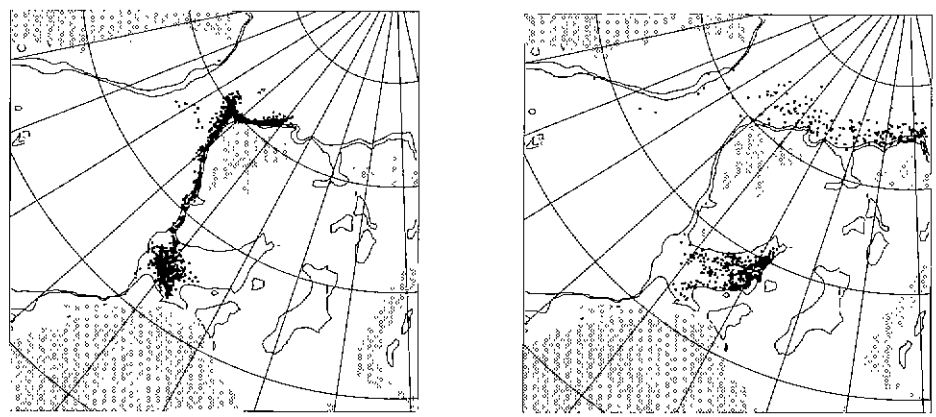

(a) 50 days

(b) 200 days

Figure 12: Particle positions with spawning over the 800 m isobath with same transport depth 300 m as in the standard run

Time	Lost	Norwegian	Barents	Greenland	Arctic
0	0	1000	0	0	0
50	0	588	180	6	226
100	0	108	357	8	527
150	146	32	372	8	442
200	378	13	374	12	223
250	486	29	357	10	118
300	546	42	342	10	60

Table 9: Number of particles with spawning at 800 m isobath

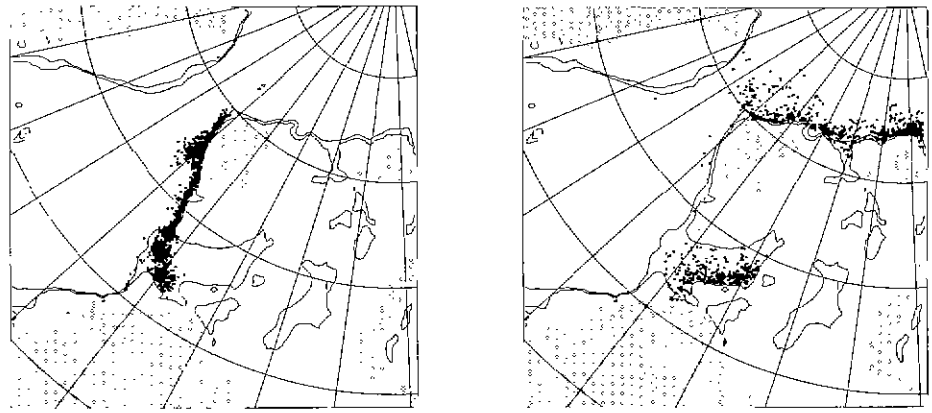

(a) 50 days (b) 200 days

Figure 13: Particle positions in 1988

Time	Lost	Norwegian	Barents	Greenland	Arctic
0	0	1000	0	0	0
50	0	889	108	0	3
100	0	423	221	1	355
150	1	195	301	2	501
200	102	33	314	2	549
250	300	26	308	2	364
300	440	19	310	3	228

Table 10: Number of particles in 1988

(averaged from December to March) is 0.25 Sv with a standard deviation of 0.65 Sv.

4 Discussion

The hydrodynamic model reproduces, at least qualitatively, the main features of the circulation in the Nordic Seas. Combined with the particle tracking model, the overall transport pattern, as presented in the standard run, looks reasonable with the particles following the Atlantic Current. The current model may underestimate the return flow in the Fram Strait area and therefore also underestimate the fraction of larvae reaching the east Greenland shelf.

The particle transport were found not to be sensitive to the spawning time. This might be expected, as the transport pattern is determined by the integrated effect of the currents over 10 months. This result justifies the use of a specific spawning date in the subsequent runs instead of the more realistic spawning curve.

The sensitivity to the transport depth is clear. The particles transported close to the surface tend to spread out over the Barents Sea, while deeper particles goes more into the Arctic and also towards Greenland. Of course, if the particles are deep enough they can not enter the Barents shelf at all.

The sensitivity studies also show that the spawning location is highly important for the

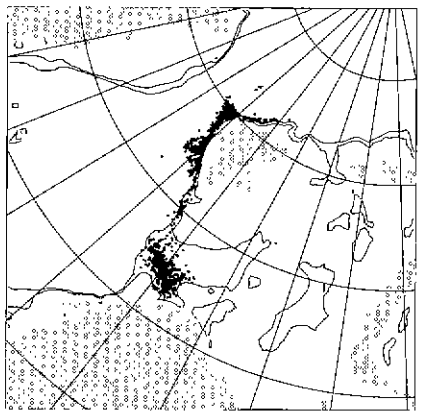

(a) 50 days

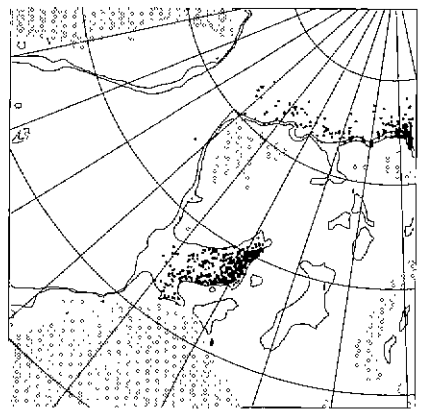

(b) 200 days

Figure 14: Particle positions in 1990

Time	Lost	Norwegian	Barents	Greenland	Arctic
0	0	1000	0	0	0
50	0	703	234	0	63
100	0	101	361	0	538
150	135	23	398	0	444
200	395	8	400	0	197
250	509	20	388	0	83
300	555	72	335	0	38

Table 11: Number of particles in 1990

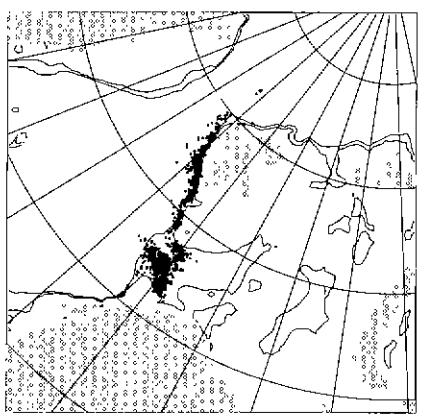

(a) 50 days

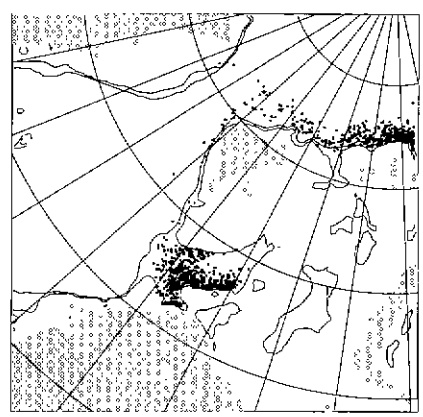

(b) 200 days

Figure 15: Particle positions in 1991

Time	Lost	Norwegian	Barents	Greenland	Arctic
0	0	1000	0	0	0
50	0	798	200	0	2
100	0	436	346	0	218
150	3	113	433	0	451
200	101	75	457	0	367
250	329	54	463	0	154
300	413	69	448	0	70

Table 12: Number of particles in 1991

Year	Norwegian	Barents	Greenland	Arctic	Inflow
1988	19	310	3	668	-0.17
1989	45	434	1	520	0.20
1990	72	335	0	593	0.40
1991	69	448	0	473	1.51

Table 13: Interannual comparison of particles category after 300 days and modelled winter inflow to the Barents Sea. The Arctic category includes here particles lost north of Franz Josef Land

modelled transport pattern. The particles released in south tends to go into the Barents Sea while the northern particles ends up in the Arctic. Spawning further offshore also reduces the number of particles in the Barents Sea and increases the number reaching the Greenland shelf.

Even if the qualitative transport patterns are similar for the years 1988-1991, the particle counts show a clear interannual variability. In table 13 this is related to the modelled wind-driven winter inflow to the Barents Sea. The low inflow in 1988 correspond to the lowest number of particles in the Barents Sea, while the extreme strong inflow in 1991 correspond to the highest Barents Sea particle count. The more normal inflow situations in 1989 and 1990 give both high and low particle counts. This suggests that strong inflow anomalies influence the relative portion of the larvae that end up in the Barents Sea. This could be investigated further by running the particle tracking for more years.

The transport modelling indicates that the area north and east of Spitsbergen may be an important nursery area for this stock. The standard runs show that 47–67% of the particles in 1988-1991 ended up in this area after 300 drifting days. Sensitivity studies with more northerly spawning or deeper transport led as much as 85–90% of the particles into this Arctic area.

The traditional survey areas in the Norwegian and Barents Seas contain 33–52% of the released particles in 1988-1991 after 300 drifting days. Although interannual variability is seen, the relative contribution of these traditional survey areas to the total particle abundance these years should have been sufficient to determine whether a recruitment failure was taken place or not. An almost absence of these yearclasses as juveniles from surveys covering these areas could therefore be justified as being indicative of bad recruitment. However, these yearclasses show up stronger as they grow older. This suggests that a larger portion of the larvae has been transported out of this area. The present modelling indicates that this is possible by

more northerly spawning and/or deeper transport.

It is also clear from this modelling work that the closer to the spawning/release time the surveys are conducted the greater the probability for encountering larvae/juveniles within the traditional survey areas within the Norwegian/Barents Seas. An optimal survey time and design must also be seen in light of the ontogeny and vertical distribution of the postlarvae.

Albert *et al.* (1997) showed that there were large inter-annual variability in the proportion of 0- and I-group Greenland halibut that were found in the Barents Sea and west of Spitsbergen respectively. The westerly distribution of 0-group off western Svalbard, and thus the suceptability of the larvae to be caught in currents towards Greenland, also varied between years. This paper shows that this inter-annual variability could, at least to some extent, be explained by variations in the current field.

The transport modelling presented here simulates only the pure physical transport of particles released at the spawning locations. If, for instance, the survival conditions in the Barents Sea and the Arctic are very different, then the particle counts will not be representative for the recruitment from the different areas. Likewise, the observed distribution patterns may also be attributable to active migrations. Greenland halibut is seldom observed during the drift phase and by the time of the 0-group surveys in autumn it is probably capable of extensive migrations.

This paper demonstrates that improved knowledge of the biology of the drift phase is needed in order to resolve these questions. The research should focus on the bathymetric distribution of Greenland halibut eggs and larvae and to inter-annual variation in the geographical distribution of spawning activity.

References

ÅDLANDSVIK, B. 1999. *LADIM User's Guide.* In preparation.

ÅDLANDSVIK, B., & LOENG, H. 1991. A Study of the Barents Sea Climate System. *Polar Research,* **10**, 45–49.

ADLANDSVIK, B., & SUNDBY, S. 1994. Modelling the Transport of Cod Larvae from the Lofoten Area. *ICES mar. Sci. Symp.*, **198**, 379–392.

ALBERT, O.T., NILSSEN, E.M., NEDREAAS, K.H., & GUNDERSEN, A.C. 1997. *Recent variations in recruitment of Northeast Atlantic Greenland halibut (Reinhardtius hippoglossoides) in relation to physical factors.* ICES CM 1997/EE:06.

ALBERT, O.T., NILSEN, E.M., STENE, A., GUNDERSEN, A.C., & NEDREAAS, K.H. 1998. *Spawning of the Barents Sea/Norwegian Sea Greenland halibut (Reinhardtius hippoglossoides).* ICES CM 1998/O:22.

ANON. 1996. *Preliminary report of the international 0-group fish survey in the Barents Sea and adjacent waters in August-September 1996.* ICES C.M. 1996/G:31. Ref. H.

BERNTSEN, J., SKAGEN, D.W., & SVENDSEN, E 1994 Modelling the transport of particles in the North Sea with reference to sandeel larvae. *Fish. Oceanogr.*, **3**, 81–91.

BLUMBERG, A.F., & MELLOR, G.L. 1987. A description of a three-dimensional coastal ocean circulation model. *In:* HEAPS, N. (ed), *Three-Dimensional Coastal Ocean Models.* Coastal and Estuarine Sciences, vol. 4. American Geophysical Union.

BOJE, J., & HAREIDE, N -R. 1993. *Trial deepwater longline fishery in the Davis Strait, May-June 1992.* NAFO SCR. Doc. 93/53, N2236.

EIDE, L.I., REISTAD, M., & GUDDAL, J. 1985. *Database av beregnede vind og bølgeparametre for Nordsjøen, Norskehavet og Barentshavet, hver 6. time for årene 1955–81.* Tech. rept. The Norwegian Meteorological Institute.

ENGEDAHL, H. 1995. Use of the flow relaxation scheme in a three-dimensional broclinic ocean model with realistic topography. *Tellus*, **47A**, 365–382.

ERIKSRØD, G., & ÅDLANDSVIK, B. 1997. *Simulation of drift of capelin larvae in the Barents Sea.* Fisken og Havet, 9: 1997, Havforskningsinstituttet.

FORRESTER, C.R., & ALDERDICE, D.F. 1973 Laboratory Observations on Early Development of the Pacific halibut. *Techn. rep. int. Pacif. Halibut Commn.*, **9**, 1–15.

GUNDERSEN, A.C., NEDREAAS, K.H., SMIRNOV, O.V., ALBERT, O T., & NILSSEN, E. 19xx. Extension of recruitment and nursery areas of Greenland halibut *Reinhardtius hippoglossoides* into the Arctic. *ICES Mar. Sci. Symp.* Submitted. Presented as a poster to the ICES Baltimore Symposium 1997.

HANSEN, B., ØSTERHUS, S., GOULD, W.J., & RICHARDS, L.J. 1998. *North-Atlantic – Norwegian Sea Exchanges. The ICES NANSEN Project.* ICES Coop. Res. Rep. No 225.

HANSEN, R., & ÅDLANDSVIK, B. 1996. *Application of a hydrodynamical model on transport of larvae of polar cod in the northern Barents Sea.* Fisken og Havet, 27: 1996, Havforskningsinstituttet.

HAUG, T., KJORSVIK, E , & SOLEMDAL, P. 1984. Vertical distribution of Atlantic Halibut (*Hippoglossus hippoglossus*) eggs. *Can. J. Fish. Aquat. Sci.*, **41**, 789–805.

HAUG, T., BJØRKE, H., & FALK-PETERSEN, I.-B. 1989. The distribution, size composition, and feeding of larval Greenland halibut (*Reinhardtius hippoglossoides* Walbaum) in the eastern Norwegian and Barents Seas. *Rapp. P.-v. Reun.Cons.int.Explor.Mer*, **191**, 226–232.

HYLEN, A., & NEDREAAS, K.H. 1995. Pre-recruit studies of the north-east arctic Greenland halibut stock. *Pages 229–238 of:* HYLEN, A. (ed), *Precision and relevance of pre-recruit studies for fishery management related to fish stocks in the Barents Sea and adjacent waters. Proceedings of the sixth IMR-PINRO Symposium, Bergen 14-17 June 1994.* Institute of Marine Research, Bergen.

ICES. 1999. *Report of the Arctic Fisheries Working Group. ICES Headquarters, 19–27 August 1998.* ICES CM 1999/ACFM:3.

LØNNING, S., KJØRSVIK, E., HAUG, T., & GULLIKSEN, B. 1982. The early development of the halibut *Hippoglossus hippoglossus (L).* compared with other teleosts. *Sarsia*, **67**, 85–92.

MELLOR, G. L., & YAMADA, T. 1982. Development of a Turbulence Closure Model for Geophysical Fluid Problems. *Rev. Geophys. Space Phys.*, **20**, 851–875.

POULAIN, P.-M., WARN-VARNAS, A., & NILLER, P.P. 1996. Near-surface circulation of the Nordic seas as measured by Lagrangian drifters. *J. Geophys. Res.*, **101**(C8), 18237–18258.

SKOGEN, M.D., MONSTAD, T., & SVENDSEN, E. 1999. A possible separation between a northern and southern stock of the northeast Atlantic blue whiting. *Fish. Res.*, **41**, 119–131.

SMIRNOV, O.V. 1995. Dynamics of Greenland halibut recruitment to the Norwegian-Barents Sea stock from 1984-1993 trawl survey data. *Pages 239–242 of:* HYLEN, A. (ed), *Precision and relevance of pre-recruit studies for fishery management related to fish stocks in the Barents Sea and adjacent waters. Proceedings of the sixth IMR-PINRO Symposium, Bergen 14-17 June 1994.* Institute of Marine Research, Bergen.

STENE, A., GUNDERSEN, A.C., ALBERT, O.T., SOLEMDAL, P., & NEDREAAS, K.H. 1999. Early development of Northeast Arctic Greenland halibut (*Reinhardtius hippoglossoides*). *J. Northw. Atl. Fish Sci.*, **25**, 1–7.

SUNDBY, S. 1983. A one-dimensional model for the vertical distribution of pelagic fish eggs in the mixed layer. *Deep Sea Research*, **30**, 645–661.

SUNDBY, S. 1991. Factors affecting the vertical distribution of eggs. *ICES mar. Sci. Symp.*, **192**, 33–38.

SVENDSEN, E., FOSSUM, P., SKOGEN, M.D., ERIKSRØD, G., BJØRKE, H., NEDREAAS, K., & JOHANNESEN, A. 1995. *Variability of the drift patterns of Spring Spawned herring larvae and the transport of water along the Norwegian shelf.* ICES C.M. 1995/Q:25.